IEEE Access
Multidisciplinary ⋮ Rapid Review ⋮ Open Access Journal

Received January 30, 2020, accepted February 29, 2020, date of publication March 4, 2020, date of current version March 13, 2020.

Digital Object Identifier 10.1109/ACCESS.2020.2978213

Numerical Simulation of the Temperature Field of Coal Subjected to Microwave Directional Heating

CHANG SU[1], YONGLI ZHANG[2], XINLE YANG[1], AND JUN TU[3]
[1]School of Mechanical Engineering, Liaoning Technical University, Fuxin 123000, China
[2]School of Mechanics and Engineering, Liaoning Technical University, Fuxin 123000, China
[3]College of Science, Liaoning Technical University, Fuxin 123000, China

Corresponding author: Yongli Zhang (zhangyl_lntu@163.com)

This work was supported in part by the National Natural Science Foundation of China under Grant 51704140, Grant 51574138, and Grant 51574136, in part by the Natural Science Foundation of Liaoning Province under Grant 2019-ZD-0040, and in part by the Foundation of Liaoning Province Education Department under Grant LJYL046.

ABSTRACT Microwave directional heating can rapidly increase the temperature of coal and promote the desorption of coalbed methane. The temperature field of coal subjected to microwave directional heating was simulated by using COMSOL software. By coupling the energy conservation equation for an electromagnetic field with the heat conduction equation for solids, a heat conduction equation for the microwave directional heating of coal was established. The effects of the microwave heating time, power, frequency, incident distance and cross-sectional area of the waveguide on the temperature field of coal were studied via simulation. The results revealed that the increasing rate of temperature was high in the early stages of microwave heating. Moreover, higher microwave power corresponded to a higher coal sample temperature, a larger temperature gradient for the coal sample, and less energy being required to achieve the desired coal sample temperature. Additionally, it was found that there is an optimal microwave frequency that maximises the temperature of the coal sample. A larger microwave incident distance resulted in a lower average coal sample temperature. The waveguide was also found to have an optimal cross-sectional area that maximises the maximum temperature of the coal sample.

INDEX TERMS Microwave, coal, directional heating, temperature field, numerical simulation.

I. INTRODUCTION

China has abundant coalbed methane resources; however, most of them exhibit low permeabilities. Improving the development and use of coalbed methane in low-permeability reservoirs will help to alleviate China's energy shortage problems, enhance the safety level of coal mine production, and reduce greenhouse gas emissions. Heat injection is a common technique applied to mine coalbed methane in low-permeability reservoirs [1]. The main methods of coalbed methane heat injection are hot-steam injection, hot-water injection, and microwave heating. Microwave heating has a high efficiency and operability [2], [3]; it has been used to study the permeability of coal and the related temperature field changes.

Microwave heating of coal can effectively promote the development of pores and fractures and increase the permeability of coal seams. The pore size, throat size, and pore numbers increase with the microwave energy [4], and microwave heating induces the increase, opening, and interconnection of pores and fractures in coal [5]. The increase in the microwave power contributes to rapid heating and thermal heterogeneity. In addition, water porosity and moisture loss increase with increasing microwave power and irradiation time [6]. With continuous exposure to microwaves, the pore size distribution of the coals extends, and the pore volume and connectivity increase [7]. Moreover, the surface area of lignite samples and mesopore percentage increase, whereas the average pore diameter and total pore volume decrease in microwave treatments [8]. The thermal stresses induced by microwave selective heating enlarge the fractures and create new cracks, thereby providing seepage space for fluids [9]. New fractures are induced in unconfined bituminous cores, and the aperture of existing cleats increases owing to high-energy microwave exposure [10].

Microwave heating of coal promotes the desorption of coalbed methane from coal; the process is highly sensitive to the excitation frequency, and higher powers cause greater thermal heterogeneity [11]. A fully coupled electromagnetic–thermal–mechanical model was developed to investigate the

The associate editor coordinating the review of this manuscript and approving it for publication was Ruilong Deng.

influence of coal compaction, thermal expansion, thermally induced gas desorption, and sorption-induced coal deformation on the coalbed methane extraction [12]. Microwave absorption by coal redistributes the electromagnetic field in the cavity, which leads to high- and low-energy regions [13]. Owing to water evaporation and thermal convection, the temperature increase in the coal sample during microwave drying exhibits a ''fast–slow–fast'' trend, and water evaporation is the key factor in the thermal distribution [14]. Moreover, the optimal frequency of 2.45 GHz achieves the maximum temperature and energy efficiency [15]. The effect of microwave frequency on temperature is clear [16]. There is just one optimal heating frequency that can achieve the maximum or minimum temperature.

The previously mentioned studies focused on heated coal samples in microwave cavities. However, the cavities required for microwave heating are difficult to construct in practical engineering projects. This limits the large-scale use of microwave cavity heating. Moreover, the position of the coal sample in the cavity influences the heating effect. Microwave directional heating has two important advantages: it does not require a cavity, and directional heating can be customized according to the desired heating direction and parameter requirements. Microwave power of 2450 MHz can be effectively applied to a bituminous pavement at a depth of up to 12 cm without overheating the top layer of the asphalt road [17]. In addition, the directional microwave technology can reduce Salmonella Enteritidis in eggshells without causing detrimental effects [18], and 4.2–4.5 GHz are optimal values for the hyperthermia treatment of dense and fatty breasts [19]. In this study, microwave directional heating was applied to the porous medium coal. Its dielectric properties differ from those of asphalt and eggshells. The temperature field of the coal sample subjected to microwave directional heating was numerically simulated, and the influence of the microwave directional heating parameters on the coal sample temperature was analyzed.

The structure of this paper is as follows: the second section presents the heat conduction equation for microwave directional heating, which was developed by coupling the electromagnetic energy conservation equation and solid heat conduction equation. The third section provides a geometric model of the numerically simulated coal sample treated with microwave directional heating, and the effectiveness of the simulation model is verified based on laboratory test analyses. In the fourth section, the simulated results are discussed to describe the effects of the microwave heating duration, power, frequency, incident distance, and cross-sectional area of the waveguide on the temperature field of the coal sample. The fifth section summarizes the paper and discusses future research directions.

II. GOVERNING EQUATIONS

Using microwaves to heat coal is a form of medium radiant heating [20]. When microwaves propagate through coal, microwave energy is converted into thermal energy by the action of the polar molecules of coal. These polar molecules are used as internal heat sources that heat the coal via an internal heat transfer process [21]. The patterns of microwave propagation through coal, and the energy convertibility of coal form the basis for studying its heat sensitivity.

The electromagnetic wave equation can be used to determine the path and range of microwave propagation in coal. The law that dictates how electric field energy is converted into thermal energy can be obtained by utilizing the electromagnetic energy conservation equation. Thus, the amount of thermal energy converted from electric field energy can be determined. Then, the solid-heat transfer equation can be coupled to establish the heat transfer model for microwave radiation in the time domain.

A. ELECTROMAGNETIC WAVE EQUATION

Let the microwaves propagate in the x direction in the coal. Then, the electromagnetic wave equation [22] is as follows:

$$\frac{\partial^2 E}{\partial x^2} = \omega^2 \varepsilon \mu (j\frac{\sigma}{\omega \varepsilon} - 1)E \tag{1}$$

where E is the electric field strength in coal; ω is the microwave frequency; ε, μ and σ are the dielectric constant, permeability and electrical conductivity of coal, respectively; j is an imaginary unit.

Then, the electric field strength in coal can be obtained by solving Equation (1)

$$E = E_{\max} \exp[-(\alpha + j\beta)x] \tag{2}$$

where $E_{\max}$ is the maximum electric field strength; x is the coordinate in the x direction; α is the attenuation constant of the electric field, and is defined as $\alpha = \sqrt{\omega\mu(\omega\varepsilon + \sqrt{\omega^2\varepsilon^2 + \sigma^2})/2}$; β is the phase constant of the electric field, and is defined as $\beta = \sqrt{\omega\mu(\omega\varepsilon - \sqrt{\omega^2\varepsilon^2 + \sigma^2})/2}$.

Apparently, α and β are determined by the characteristic parameters of coal, and the microwave frequency. Alternatively, $E_{\max}$ is determined by the microwave power. According to the definition of power, the amount of energy provided by the microwave source to the coal per unit time is

$$Q = \varepsilon E_{\max}^2 = \frac{P}{vS} \tag{3}$$

where P is the microwave power; S is the cross-sectional area of the waveguide; v is the wave velocity of the microwaves in coal. Here, $v = C/\sqrt{\varepsilon\mu}$, where C is the speed of light, which is given as $C = 3 \times 10^8$ m/s.

Following substitution, it is easy to obtain

$$E_{\max} = \sqrt{\frac{P}{SC}\sqrt{\frac{\mu}{\varepsilon}}} \tag{4}$$

Then, by substituting Equation (2) into Equation (4), the distribution equation for the electric field in coal can be obtained as

$$E = \sqrt{\frac{P}{SC}\sqrt{\frac{\mu}{\varepsilon}}} \exp[-(\alpha + j\beta)x] \tag{5}$$

B. ENERGY CONVERSION EQUATION

The energy conservation equation for an electromagnetic field [23] is given as

$$\int_V J \cdot E dV + \int_V j\omega(\varepsilon E^2 + \mu H^2) dV + \int_V \nabla \cdot (E \times H) dV = 0 \tag{6}$$

where H is the magnetic field strength; V is unit volume; J is the current density; ∇ is the Hamilton operator.

The first integral on the left side of Equation (6) represents the amount of electromagnetic energy that is converted by coal into Joule heat energy. The second integral on the left side of Equation (6) represents the amount of electromagnetic energy that is consumed by coal. The third integral on the left side of Equation (6) represents the amount of electromagnetic energy that is input into coal.

In addition to Joule heat energy that is converted by coal, the polarisation loss of electromagnetic waves in coal also generates heat when the coal is heated by microwaves. In the second integral on the left side of Equation (6), $\varepsilon = \varepsilon_0 \varepsilon_r$, where ε_r is the relative dielectric constant, and $\varepsilon_0 = 8.85 \times 10^{-12}$ F/m. Furthermore, ε_r is described as a complex quantity with real and imaginary parts, and is denoted as $\varepsilon_r = \varepsilon' - j\varepsilon''$. The real part, ε', is the dielectric constant of coal. The imaginary part, ε'', is typically used to describe the polarisation loss, and is referred to as the loss factor.

By taking into account $J = \sigma E$ and substituting the complex dielectric constant ε, we can rewrite Equation (6) as

$$\int_V (\omega\varepsilon_0\varepsilon'' + \sigma) E^2 dV + \int_V j\omega\varepsilon_0\varepsilon' E^2 dV + \int_V j\omega\mu H^2 dV + \int_V \nabla \cdot (E \times H) dV = 0 \tag{7}$$

The first integral on the left side of Equation (7) yields the total amount of thermal energy that is converted from microwave energy. Therefore, the amount of heat energy that is generated by the microwaves in the coal is given as

$$Q_e = (\omega\varepsilon_0\varepsilon'' + \sigma) E^2 \tag{8}$$

By incorporating the electric field distribution Equation (5) into Equation (8), we can obtain the thermal energy distribution in coal

$$Q_e = (\omega\varepsilon_0\varepsilon'' + \sigma) \frac{P}{SC} \sqrt{\frac{\mu}{\varepsilon}} \exp[-2(\alpha + j\beta)x] \tag{9}$$

C. HEAT TRANSFER EQUATION

Owing to the volatility of microwaves and the attenuation of energy that is caused by their propagation, the distribution of thermal energy in coal is non-uniform. Therefore, heat conduction occurs within the coal sample. The first law of Thermodynamics [24] is given as

$$\rho C_p \frac{\partial T}{\partial t} + \rho C_p u \cdot \nabla T = \nabla \cdot (k \nabla T) + Q_e \tag{10}$$

where ρ, C_p and k are the density, heat capacity and thermal conductivity of the coal, respectively; u is the rate of temperature change in space as a function of time; ∇T is the temperature gradient.

By incorporating Equation (9) into Equation (10), we can obtain the heat transfer model for microwave directional heating in the time domain, which is given as

$$\rho C_p \frac{\partial T}{\partial t} + \rho C_p u \cdot \nabla T = \nabla \cdot (k \nabla T) + (\omega\varepsilon_0\varepsilon'' + \sigma) \frac{P}{SC} \sqrt{\frac{\mu}{\varepsilon}} \exp[-2(\alpha + j\beta)x] \tag{11}$$

The first term on the left side of Equation (11) describes the relationship between temperature and time. The second term on the left side of Equation (11) describes the relationship between temperature and space. The first term on the right side of Equation (11) describes the heat transferred from the external environment.

For the coal sample that was used in this study, ε, ε_0, ε'', C_p, ρ, μ, σ and k in Equation (11) are constants that cannot be changed. Thus, we should focus on the controllable parameters. In fact, there are four controllable parameters in Equation (11), i.e., the microwave heating time t, microwave power P [25], microwave frequency ω, and cross-sectional area of the waveguide S. In addition, the incident distance of the microwaves directly affects the energy of the microwaves penetrating the coal sample. The incident distance of the microwaves is defined as the distance between the edge of the near-waveguide of the coal sample and the output port of the waveguide, and is denoted as d.

III. SIMULATION MODEL

A. BASIC ASSUMPTIONS

Although there are differences between the real-world conditions and the corresponding numerical model, a numerical simulation can be used to intuitively demonstrate the respective influences of various factors. Particularly, some important parameters cannot be measured in the laboratory, such as the distribution of the temperature field within the coal sample. Therefore, a numerical simulation was performed in this study to investigate the distribution of the temperature field within a coal sample that is subjected to microwave directional heating. To optimise computational and CPU usage efficiency, the following assumptions were made. 1) The coal sample is homogeneous and isotropic. 2) The thermophysical and dielectric properties are constant. 3) Mass transfer is negligible. 4) There is no heat conduction within the air or coal sample.

B. GEOMETRIC MODEL

The geometry of the microwave directional heating model for a coal sample is shown in Figure 1. The waveguide output faced the coal sample, and the microwaves were set to penetrate the waveguide from the incident port. The waveguide material was copper. A virtual air hood was designed to

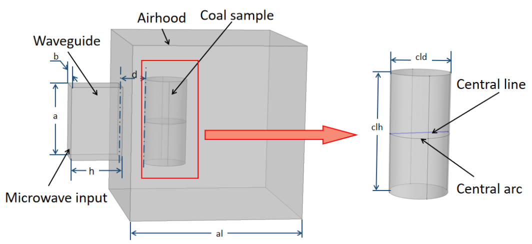

FIGURE 1. Geometry of microwave directional heating.

surround the coal sample to limit the feasible range for the electromagnetic field.

The basic parameters of the geometric model are provided in Table 1.

TABLE 1. The basic parameters of geometric model.

Symbol	Description	Value [mm]
a	waveguide depth	86
b	waveguide height	43
h	waveguide width	50
d	incident distance	5
al	airhood length	200
cld	coal sample diameter	50
clh	coal sample height	100

C. BOUNDARY CONDITIONS

In the geometric model shown in Figure 1, microwaves enter the rectangular waveguide from the microwave incident port, which was set as the excitation port. Additionally, the rectangular waveguide operates in TE10 mode. The power flow of the microwaves satisfies

$$s = \frac{\int_{\partial\Omega}(E - E_1)\cdot E_1}{\int_{\partial\Omega} E_1 \cdot E_1} \tag{12}$$

where E_1 is the electric field strength of the incident port in TE10 mode.

A standard waveguide is made of aluminium. Thus, to minimise surface erosion, the inner wall of the waveguide was coated with a highly conductive copper layer. The complex reflection index of the copper layer was set as $|N| \gg 1$. The boundary condition for the waveguide was set as the impedance boundary condition. This condition can be mathematically described as follows:

$$\sqrt{\frac{\mu_0\mu_r}{\varepsilon_0\varepsilon_r - \frac{j\sigma}{\omega}}}\, n\times H + E - (n\cdot E)n = (n\cdot E_s)n - E_s \tag{13}$$

where E_s is the electric field source that is used to specify a surface current source at the boundary; n is the normal vector of the boundary; μ_0 and μ_r are the permeability of the vacuum and relative permeability, respectively.

In accordance with the operating mode of a rectangular waveguide, the electric field strength in the y direction is

$$E_{0y} = \sin(\frac{\pi x}{a}) \tag{14}$$

where a is the waveguide depth.

The propagation constant for microwaves in the waveguide is

$$\beta_0 = \frac{2\pi}{C}\sqrt{f^2 - f_c^2} \tag{15}$$

where f is the line frequency; f_c is the cut-off frequency of the rectangular waveguide, and $f_c = C/(2a)$.

The waveguide and air hood were designed to form a closed cavity that defines the simulated area. The medium in the air hood was set to be ambient air. Then, the air hood boundary was set to mimic the conditions of an ideal magnetic conductor; this can be described as follows:

$$n \times H = 0 \tag{16}$$

The current density at the surface boundary was set to equal 0. The magnetic field on both sides of the air hood was designed to be continuous. Additionally, in the proposed model, there is no reflection of microwaves in the air hood, ensuring that the microwaves can only be transmitted in the desired direction.

D. EXPERIMENTAL VERIFICATION

The investigated experimental system is shown in Figure 2. It consists of a microwave generator, waveguide, microwave shield, and thermograph.

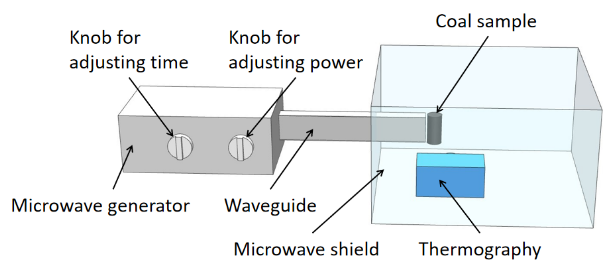

FIGURE 2. Experimental microwave directional heating system.

The microwaves were generated by a common microwave generator, and a standard waveguide directed the microwaves into the coal sample (waveguide standard: WR-340 model). The microwave shield was a wooden crate that was humidified before the experiment to prevent microwave leakage and to ensure the safety of the researchers and equipment. The surface temperature of the coal sample was measured with a thermograph (VarioCAM hr (InfraTec) thermal imaging camera).

The experimental coal sample originated from the low-permeability coal seam of the Fuxin Wulong Mine in China. Coal has primitive and complex pore and fissure structures, and the internal composition distribution is inhomogeneous, which causes strong interference in the microwave heating results. Therefore, the coal sample was ground and sieved to eliminate the reflection and scattering interference caused by microwave propagation in the original pore fissures. The resulting homogeneous coal sample exhibited a consistent temperature change trend under microwave heating.

The 60–80 mesh pulverized coal powder was subjected to compression molding to prepare a coal sample with a diameter of 50 mm and height of 100 mm, such as in [15]. The determined properties are listed in Table 2 for an initial temperature of 23 °C.

TABLE 2. Thermal and electrical properties of coal sample.

Symbol	Material property	Value	Unit	Sources
ε_r	Relative permittivity	3 − 0.15j	1	Experiments
μ	Relative permeability	1	1	[12]
ρ	Density	1263	kg/m^3	Experiments
σ	Electrical conductivity	0.001	S/m	Experiments
k	Thermal conductivity	0.478	W/(m·K)	[12]
C_p	Heat capacity at constant pressure	1000	J/(kg·K)	[12]
T_0	Initial temperature	23	°C	Experiments

To verify the effectiveness of the simulation model, microwave directional heating experiments were performed on the selected coal sample in a laboratory. The frequency of the generated microwaves was 2.45 ± 0.05 GHz, and the microwave output power of the experimental system was 700 W. The incident distance of the microwaves was 1 mm, cross-sectional area of the microwave waveguide was 86 × 43 mm^2, and heating duration was 180 s. The properties of the coal sample and experimental parameters were implemented in the simulation model with the COMSOL software.

To compare the experimental and simulated results, points L and R were selected on the outer surface of the coal sample. They are the closest and farthest points from the waveguide on the central axis of the microwave propagation direction, respectively. Figure 3 shows the temperature changes at the two points over time.

Figure 3 compares the simulated and experimental results of Points L and R. Both simulated and experimental temperatures of the coal samples showed a monotonous increase with increasing heating duration. However, the simulated temperature exhibited a linear increase and the experimental temperature a nonlinear increase. This was mainly due to the existence of interference factors during the experiment, such as the heat transfer between the coal sample and environment and the change in the dielectric constant of the coal sample. When the coal sample temperature was low (below 80 °C), the simulated results agreed well with the experimental results. The small deviation between the simulated

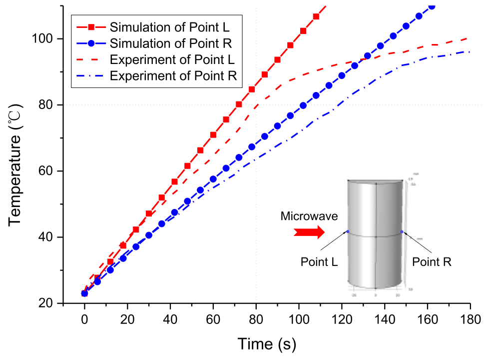

FIGURE 3. Temperature changes at Points L and R.

and experimental results was mainly due to the heat transfer between the coal sample and environment, which was not considered in the simulation. However, when the coal sample temperature was high, the simulated temperature curve was significantly higher than the experimental temperature curve, and the difference increased sharply. The main reason for this phenomenon was that the dielectric constant of coal changes dramatically with the temperature when the temperature of the coal sample is high [26].

Considering the economics of coalbed methane extraction by microwave heating and the changes in the coal matrix chemistry due to excessively high temperatures, the authors believed that it was appropriate to limit the maximum temperature to which the coal samples were heated. Consequently, it could be assumed that the dielectric constant of coal does not change in the simulation. In this study, the temperature limit was set to 80 °C by limiting the coal sample heating time and microwave power. Several researchers have reported that when the temperature of a coal sample is low, the change in the dielectric constant of coal is not evident [26]. Under the presented parameter settings, when the coal sample was heated for 80 s, the maximum temperature of the coal sample was approximately 85 °C. Therefore, the temperature of the central arc on the surface of the coal sample after it had been heated for 80 s was investigated; the results are shown in Figures 4 and 5, respectively.

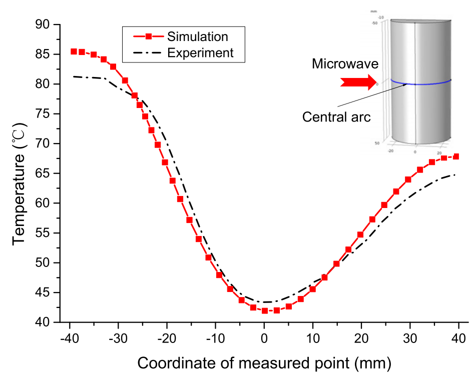

FIGURE 4. Temperature of central arc of coal sample surface.

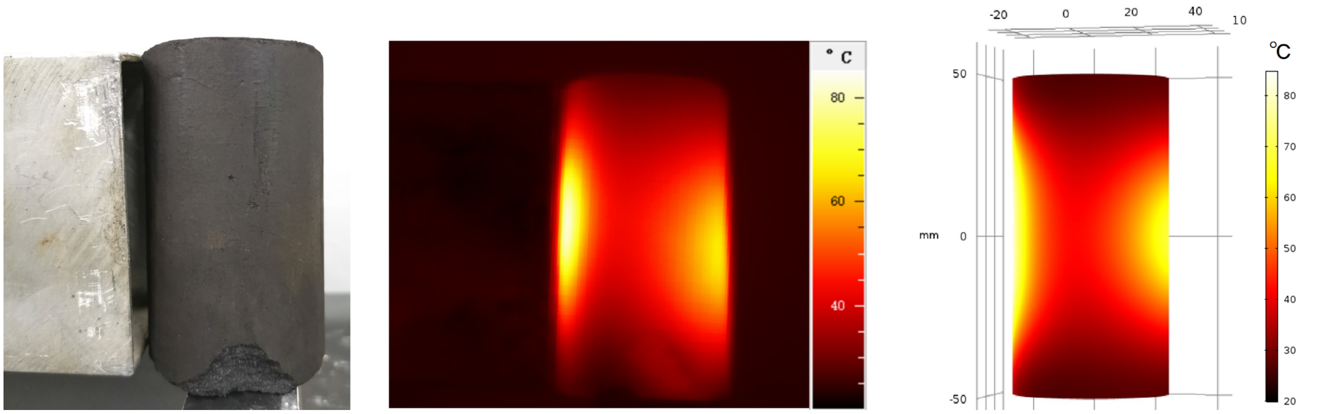

(a) (b) (c)

FIGURE 5. Temperature of surface: (a) coal sample; (b) thermal imaging map of experiment; (c) cloud map of simulation.

Figure 4 presents the temperature distribution of the central arc on the surface of the coal sample after it had been directionally heated for 80 s. The simulated and experimental temperatures at each point on the central arc agree well. They decreased first and then increased with respect to the coordinate. On the central axis of the microwave propagation direction, the temperature of Point L (closest to microwave source) was the highest, and the temperature of Point R (farthest from microwave source) was the second highest. The temperature of the tangent point of the microwave propagation direction and the central arc was the lowest.

Furthermore, Figure 4 shows a small deviation between the simulated and experimental temperatures of the central arc. This was mainly due to the heat transfer between the coal sample and environment in the experiment, which was not considered in the simulation. When the measured point temperature was relatively high, the simulated temperature was higher than the experimental temperature. When the measured point temperature was relatively low, the simulated temperature was lower than the experimental temperature. The high-temperature part of the coal sample transmitted heat into air, and the air transmitted heat to the low-temperature part of the coal sample. The greater the deviation between the coal sample temperature and environmental temperature, the greater was the deviation between the simulated and experimental results. Considering that heat transfer was the main cause of the deviation between the simulated and experimental results, Figure 4 also verifies that when the coal sample temperature was low, the dielectric constant of the coal did not change significantly.

To estimate the heat transfer between the coal samples and environment, Points L and R are taken as examples. After microwave directional heating for 80 s, the simulated and experimental temperatures at Point L were 85.4 and 81.2 °C, and the simulated and experimental temperatures at Point R were 67.8 and 64.7 °C, respectively. Because the initial temperature of the coal sample was 23 °C, the temperature difference between Points L and R due to the heat transfer were 4.2 and 3.1 °C, respectively. In other words, the simulated temperatures of Points L and R without considering the heat transfer were 7.2% and 7.4% higher than the experimental temperatures, respectively. It should be pointed out that the heat transfer between the coal sample and environmental air inside the coal sample was less than that on the coal surface. Therefore, the heat transfer between the coal samples and environmental air was not considered in the following simulations.

Figure 5(a) presents the coal sample used for the experiment, and Figure 5(b) is a thermal imaging image of the surface of the coal sample after an 80 s heating treatment (experiment). In addition, Figure 5(c) presents a cloud map of the surface temperature of the coal sample after an 80 s heating treatment (simulation). The results show that the distributions of hot and cold spots produced by the simulated cloud map are consistent with those of the thermal imaging map. In addition, the temperature of the hot spot on the left side was higher than that of the hot spot on the right side. However, the area of the hot spot on the left side was smaller. Consequently, the temperature variation of the hot spot on the left side was higher than that of the hot spot on the right side.

The simulated results agree well with the experimental ones for the temperature variation at the central arc of the coal sample and the temperature distribution on the surface. The simulated temperature field distribution of a coal sample that has been subjected to microwave directional heating is discussed in the following section.

IV. ANALYSIS OF RESULTS

In the simulation, the effects of the time, power, frequency, incident distance, and cross-sectional area on the temperature distribution of the coal sample subjected to microwave directional heating were studied. The values of the basic parameters were set as follows: $t = 80$s, $P = 700$ W, $f = 2.45$ GHz, $d = 1$ mm, and $S = 86 \times 43$ mm^2, which correspond to the parameters of the experimental verification.

A. INFLUENCE OF TIME

The duration of microwave heating was found to affect the temperature profile of the coal sample directly. Specifically, large temperature fluctuations can generate and expand the pores and fissures within the coal sample, eventually affecting the permeability of the coal sample [27]. The effects of microwave heating duration on the temperature of the coal sample are shown in Figure 6. It can be seen that the values for the temperature difference at the measured points yielded a V shape over periods of 10 s. To provide a better description, we separated the curve in Figure 6 into three regions that have been respectively labelled as I, II and III. Regions I and III are peak regions with large temperature fluctuations, whereas Region II is a valley region with small temperature fluctuations. This is consistent with the patterns of microwave propagation through the implemented medium.

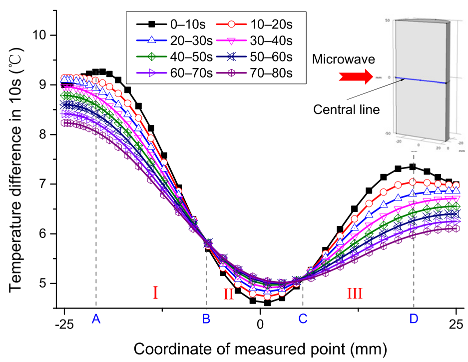

FIGURE 6. Temperature difference on the central line.

As the heating duration increased, the extent of temperature fluctuation at the measured points in Regions I and III decreased every 10 s. The most significant temperature variation occurred between 0 and 10 s, and the smallest temperature variation was found to occur between 70 and 80 s. The effects of heating duration on temperature variation in Region II were not significant. As the coordinate value of the measured point in Region I increases, the temperature variation of the measured point within any 10-s time span decreases. The temperature fluctuations at the measured point in Region II were small over every 10-s period. In Region III, the location of the measured point significantly influenced the temperature in the early stage of heating; however, the influence of measured point location on the temperature variation was not significant in the late stage of heating.

The four points A, B, C, and D on the central line of the coal sample were chosen (Figure 6). At Points A and D, the difference in the temperature change during 10 s was the largest. At Points B and C, the temperature change remained approximately constant. In addition, the changes in the temperature with respect to the time are shown in Figure 7.

Points A and D exhibited the same negative temperature change. The largest temperature fluctuations were observed immediately after the beginning of the heat treatment. Then, the negative slope increased rapidly. The variation trends for

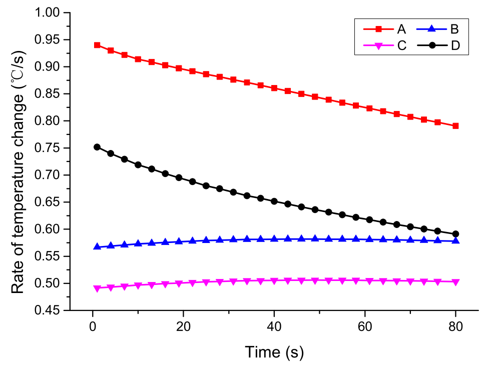

FIGURE 7. Rate of temperature change.

Points B and C were consistent: the temperature change was insignificant. Because Point A was closer to the microwave source than Point D, the temperature change rate at Point A was consistently higher than that at Point D. This is because polar molecules in the coal sample absorbed some of the microwave energy, which decreased the energy at the second peak position.

B. INFLUENCE OF POWER

Power is an important parameter of the microwave source, as it describes how fast the microwave source outputs energy. Whether the heating efficiency of the coal sample can be improved by changing the power is an important consideration for engineering applications. For this reason, eight output power values were investigated in this study, i.e., 50, 100, 200, 300, 400, 500, 600 and 700 W. The coal sample was heated by applying microwave energy for 80 s; the results are shown in Figure 8.

Figure 8(a) shows that the maximum and average temperatures of the coal sample increased with increasing power. It can be seen that the minimum temperature was not significantly affected by the amount of power. When the heating time was fixed, increasing the microwave output power led to the coal sample having higher maximum and average temperatures. In addition, the maximum temperature was found to be more affected by the power of the microwave source than the average temperature.

The temperature cloud map presented in Figure 8(b) shows that the temperature and radius of the hot spot increased with an increasing amount of power. This indicates that the temperature and heated area of the coal sample were positively correlated with the microwave power. Thus, the microwave power can be increased to obtain a higher heating temperature and wider heating range.

High-power microwaves can rapidly increase the coal sample temperature; however, this process consumes a relatively large amount of energy per unit time, which is not cost-effective for industrial production. Considering this, we investigated the relationship between energy and temperature as a function of output power. The results are shown in Figure 9.

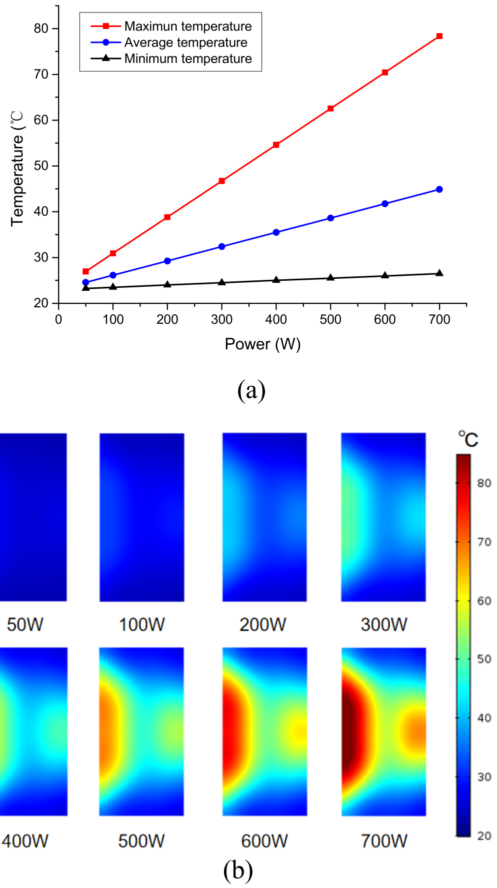

FIGURE 8. **Effect of power on temperature: (a) temperature curve; (b) temperature distribution.**

Figure 9(a) shows that the average temperature of the coal sample gradually increased with increasing microwave output energy. However, microwave power was found to have a positive effect on the increase in average temperature. Specifically, more power corresponded to a faster average temperature increase. When the amount of energy was fixed, more power corresponded to a higher average temperature of the coal sample. However, increasing the output power of the microwave energy resulted in the coal sample requiring less energy to reach the target temperature. For example, the amount of energy required for the 700-W microwave source to heat the coal sample to 80 °C was 49.99% of that required for the 50-W microwave source. This means that a high-power microwave source is more economical than a low-power microwave source.

The temperature cloud map in Figure 9(b) shows that the centre position and radius of the hot spot were not affected by the amount of power. Conversely, the temperature of the hot spot differed according to the amount of power. When the microwave power was 700 W, the temperature and visibility of the hot-spot boundary were maximised. Moreover, the largest difference between the maximum and minimum temperatures was observed. This means that the output power directly affects the temperature gradient within the coal sample.

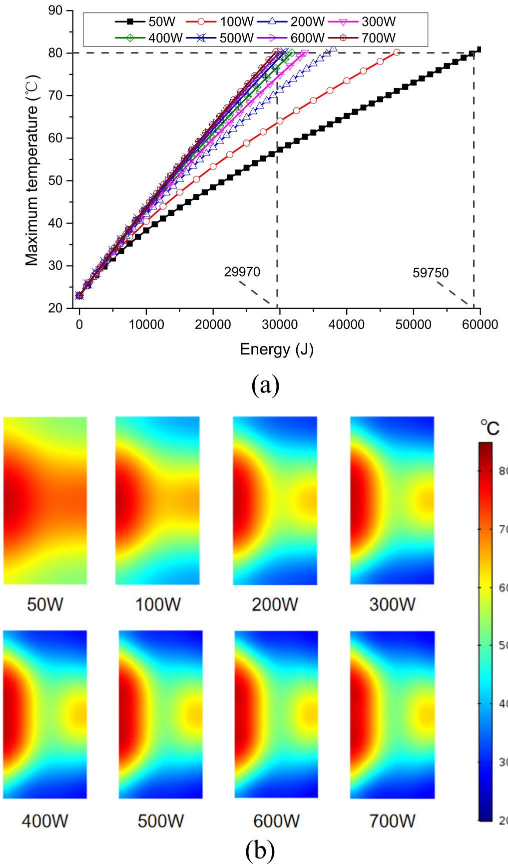

FIGURE 9. **Effect of power on average temperature: (a) temperature curve; (b) temperature distribution.**

The temperature gradient within the coal sample was found to affect the thermal stress directly. Specifically, when the thermal stress exceeded the tensile strength of the coal sample, the internal microstructure structure of the coal sample was broken, consequently changing the permeability of the coal sample. Figure 10 shows the relationship between the temperature gradient of the coal sample and the microwave power.

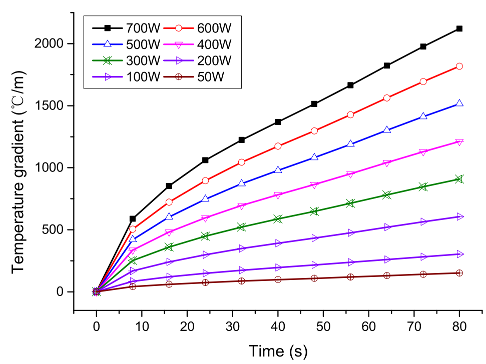

FIGURE 10. **Effect of power on temperature gradient.**

The temperature gradient increased with the power (Figure 10). In addition, the microwave power was the most significant determinant of the maximum temperature (Figure 8). The temperature gradient increased rapidly in the early stage of the heat treatment. Subsequently, it increased gradually. The rate at which the temperature gradient changed differed according to the power.

C. INFLUENCE OF FREQUENCY

The frequency of an industrial microwave oven can be 0.915 or 2.45 GHz, which is determined by the optimal heating frequency of the water molecules. However, these two frequencies may be non-optimal for coal samples. To determine the optimal microwave frequency for coal samples, the heating effect of microwaves with frequencies in the range of 0.915–10 GHz was simulated. Figure 11 shows the temperature curve and distribution for the coal sample.

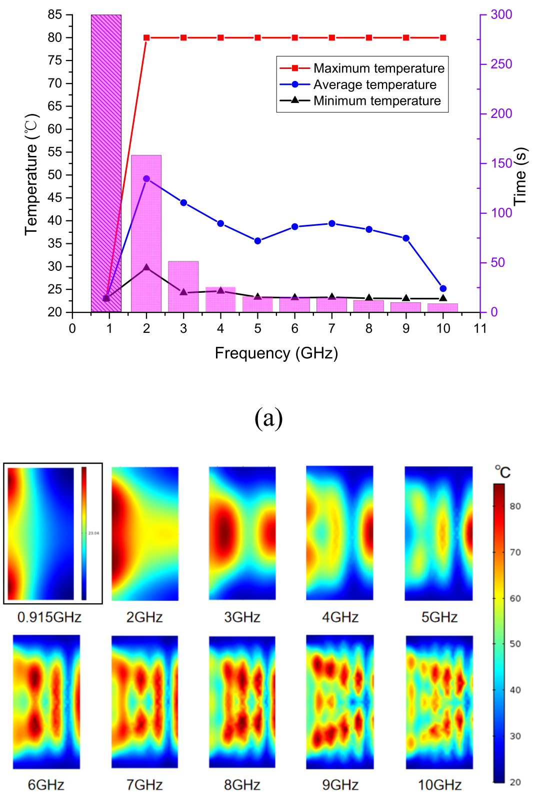

FIGURE 11. Effect of frequency on temperature: (a) temperature curve; (b) temperature distribution.

The time required for the microwave-heated coal samples at different frequencies to reach the maximum temperature of 80 °C is shown in Figure 11(a). The microwave with a frequency of 0.915 GHz could not heat the coal sample to 80 °C within the acceptable simulation time (it was estimated to take approximately 200 h). Therefore, a different legend is presented in the figure. The higher the microwave frequency, the less time it took for the temperature of the coal sample to reach °C. To reach 80 °C, microwaves with a frequency of 2 GHz need 158 s, whereas microwaves with a frequency of 10 GHz need only 8.2 s. For a maximum temperature of the coal samples of 80 °C, the average temperature of the coal samples corresponding to different frequency microwaves was different. The 2 GHz microwave maximized and the 10 GHZ microwave minimized the average temperature. However, the variation in the average temperature of the coal samples with respect to the frequency was not monotonic. In addition, the effect of the different frequency microwaves on the minimum temperature of the coal samples was not significant. Interestingly, the 2 GHz microwave also maximized the minimum temperature.

According to the temperature distribution in Figure 11(b), increasing the frequency significantly affected the hot spot. With increasing frequency, the diameters and spacings of the hot spots decreased gradually, and the number of hot spots increased gradually. When the frequency was 0.915 or 2 GHz, the two hot spots were arranged vertically, and a hot spot with a large diameter was formed. However, when the frequency was 3, 4, or 5 GHz, the diameters of the hot spots became smaller, and they aligned horizontally. Over 6 GHz, hot spots were generated in both horizontal and vertical directions, which increased gradually with increasing frequency.

At 0.915 GHz, the hot spot position was only on the left side of the coal sample, and the heating range was very small. When the frequency increased to 2 GHz, the heating area of the coal samples along the horizontal direction increased with increasing frequency. Thus, the higher the frequency, the larger was the microwave heating range inside the coal sample. The increasing frequency reduced the diameter of the hot spot and caused the overall average temperature to decrease.

The influence of the microwave frequency on the temperature of the coal sample in Figure 11 is interesting for the following reasons. When the microwave frequency was relatively low (i.e., 0.915 GHz), the polar molecules of the coal sample vibrated slowly because less microwave energy was converted into heat, and a large amount of microwave energy that reached the coal sample was lost to the surrounding air. This explanation is supported by the fact that the temperature of the coal sample did not significantly change. As the microwave frequency increased from approximately 2 to 5 GHz, the vibration of the polar molecules of the coal sample intensified. The amount of thermal energy that was converted increased, and the amount of microwave energy lost to the surrounding air decreased. These results were evidenced by the simultaneous increase in the minimum and maximum temperatures of the coal sample. Then, in the highest microwave frequency range (i.e., 6–10 GHz), the intensity of the polar molecule vibrations increased significantly. The temperature in the hotspot area increased rapidly to 80 °C. At the same time, the decrease in the hot spot diameter reduced the minimum temperature of the coal samples outside the heated area, thereby resulting in a gradual decrease in the average temperature.

D. INFLUENCE OF INCIDENT DISTANCE

The distance between the microwaves used for directional heating and the coal sample should be small. Because microwaves tend to propagate through a medium in the form of a plane wave, the incident distance of the microwaves affects directly the amount of microwave energy that penetrates the coal sample. The relationship between the incident distance and temperature of the coal sample after an 80 s microwave heat treatment is shown in Figure 12.

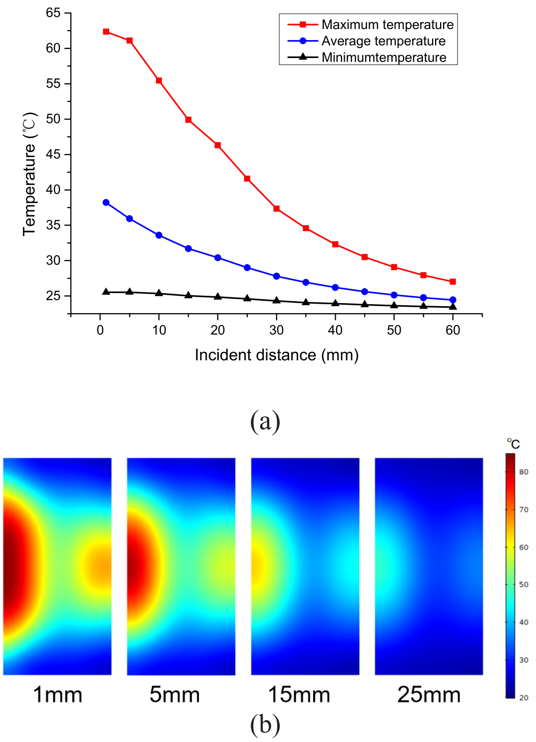

FIGURE 12. Effect of microwave incident distance on temperature: (a) temperature curve; (b) temperature distribution.

According to Figure 12(a), the changes in the temperature of the coal sample were influenced by the incident distance. All three temperatures of the coal sample decreased with increasing incident distance. Specifically, the maximum and average temperatures of the coal sample were significantly affected by the incident distance. In addition, the minimum temperature was moderately affected by the changes in the incident distance.

When the incident distance was 1 mm, the temperature of the coal sample hot spot was significantly higher than that with an incident distance of 25 mm; the results are shown in Figure 12(b). The shorter the incident distance, the higher the temperature of the hot spot. Thus, a shorter incident distance for the microwaves corresponds to a larger heated zone of the coal sample. When the incident distance was too long, more microwave energy was lost, and the temperature of the coal sample decreased significantly. Hence, a shorter microwave incident distance resulted in more highly concentrated microwave energy penetrating the coal sample and a higher maximum temperature.

E. INFLUENCE OF CROSS-SECTIONAL AREA

Because the coal sample was directionally heated by the microwaves, the energy was transmitted to the coal sample through a rectangular waveguide. Thus, the size of the cross-section of the rectangular waveguide affected the heat treatment directly. According to the standard rectangular waveguide settings, the height of a waveguide is half its depth, which is denoted as a. Thus, the cross-sectional area of a rectangular waveguide can be defined as $S = a^2/2$. The relationship between the cross-sectional area of the waveguide and temperature is illustrated in Figure 13.

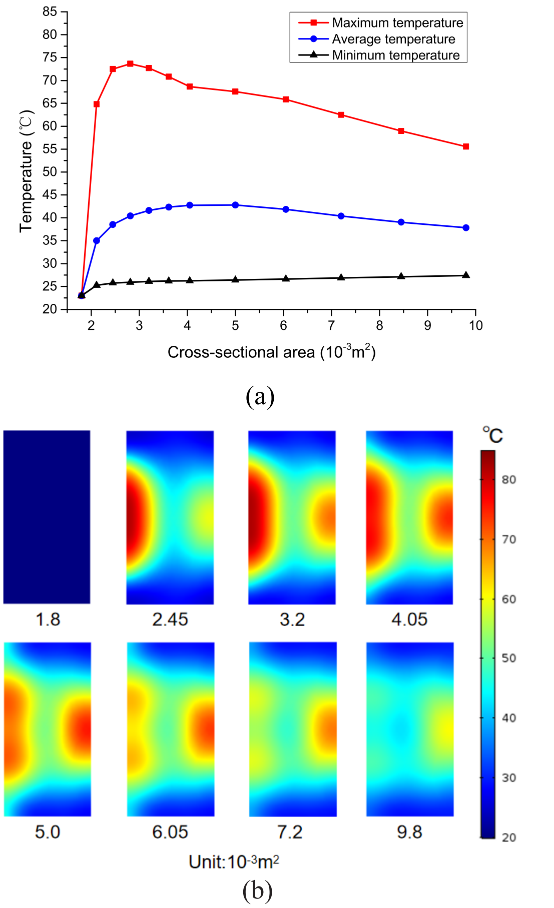

FIGURE 13. Effect of cross-sectional area of microwave on temperature: (a) temperature curve; (b) temperature distribution.

Figure 13(a) shows that the maximum and average temperatures of the coal sample initially increased, and then decreased as the cross-sectional area of microwave waveguide increased. In particular, the influence of the cross-sectional area of the waveguide on the maximum temperature was more significant than its influence on the average temperature. Conversely, the influence of the cross-sectional area of the waveguide on the minimum temperature was not significant. It can also be seen that the maximum temperature reached its maximum value when the cross-sectional area of the waveguide was 0.0028 m^2. Beyond this value, the maximum temperature decreased with increasing cross-sectional area of the microwave waveguide. The reason for this phenomenon is as follows. As the depth of the waveguide increased, its cross-sectional area gradually approached the cross-sectional area of the coal sample. Consequently, the amount of energy lost via the waveguide increased. More specifically, when the cross-sectional area of the waveguide exceeded the cross-sectional area of the coal sample, the amount of microwave energy substantially decreased, and the maximum temperature of the coal sample rapidly decreased.

Figure 13(b) shows that the number and location of hot spots were not dependent on the cross-sectional area of the waveguide. However, the maximum temperature of the hot spots initially increased, and then began decreasing, as the cross-sectional area of the waveguide increased. Moreover, as the cross-sectional area of the waveguide increased, the size of the two hot spots gradually increased, and the two hot spots gradually merged. Therefore, a larger waveguide cross-sectional area led to a more uniform microwave heat treatment being applied to the coal sample.

In summary, it is necessary to optimise the cross-sectional area of the waveguide to maximise the maximum temperature for practical engineering applications. However, to achieve better heating uniformity, the cross-sectional area of the waveguide can be increased.

The simulation results serve as guidance for the parameter selection of microwave directional heating treatments for coal. For example, to increase the maximum temperature of the coal sample, the heating duration, heating power, and microwave frequency can be increased; the incident distance can be decreased; or an appropriate waveguide cross-sectional area can be selected.

V. CONCLUSION

In consideration of the efficacy and cost-effectiveness of applying microwave directional heating to coal, the temperature field of a coal sample subjected to microwave directional heating was numerically simulated using COMSOL software. By coupling the electromagnetic field energy conservation and solid heat conduction equations, a heat conduction equation for a coal sample subjected to microwave directional heating was derived. According to the characteristic conditions of microwave directional heating, a geometric model was constructed, and the boundary conditions were determined. By comparing the laboratory-based experimental results to the simulated results, we proved that the simulation model is effective. Furthermore, the simulated results were used to investigate the effects of microwave heating duration, power, frequency, incident distance and waveguide cross-sectional area on the temperature field of the coal sample.

The results show that the temperature change in the coal samples with increasing heating time was complicated. The temperature change rate in the microwave propagation direction showed a wavy distribution, and the temperature change rate of the peak in the earlier stage of the microwave heating treatment was greater than that in the later stage. The microwave power affected the temperature of the coal samples positively: the greater the power, the less energy was required to reach the target temperature. Moreover, the temperature gradient increased with the power, and the microwave frequency exhibited a threshold. Microwaves above the threshold frequency heated the coal samples quickly, and the heating time decreased with the frequency. Specifically, the microwave frequency affected the internal temperature distribution of the coal samples, and higher frequencies created more hot spots inside the coal samples. The shorter the microwave incident distance, the higher was the temperature of the coal sample. In addition, there was a suitable area for the incidence cross-sectional area. In general, the influences of the heterogeneous coal dielectric constant and coal sample size on the microwave directional-heating treatment results of coal should be studied further.

REFERENCES

[1] Q. Zou, B. Lin, C. Zheng, Z. Hao, C. Zhai, T. Liu, J. Liang, F. Yan, W. Yang, and C. Zhu, "Novel integrated techniques of drilling–slotting–separation-sealing for enhanced coal bed methane recovery in underground coal mines," *J. Natural Gas Sci. Eng.*, vol. 26, pp. 960–973, Sep. 2015.

[2] E. Binner, E. Lester, S. Kingman, C. Dodds, J. Robinson, T. Wu, P. Wardle, and J. P. Mathews, "A review of microwave coal processing," *J. Microw. Power Electromagn. Energy*, vol. 48, no. 1, pp. 35–60, May 2016.

[3] W. Wei, Z. Shao, Y. Zhang, R. Qiao, and J. Gao, "Fundamentals and applications of microwave energy in rock and concrete processing—A review," *Appl. Therm. Eng.*, vol. 157, Jul. 2019, Art. no. 113751.

[4] Y.-D. Hong, B.-Q. Lin, C.-J. Zhu, and H. Li, "Effect of microwave irradiation on petrophysical characterization of coals," *Appl. Therm. Eng.*, vol. 102, pp. 1109–1125, Jun. 2016.

[5] H. Li, S. Shi, J. Lu, Q. Ye, Y. Lu, and X. Zhu, "Pore structure and multifractal analysis of coal subjected to microwave heating," *Powder Technol.*, vol. 346, pp. 97–108, Mar. 2019.

[6] J. Huang, G. Hu, G. Xu, B. Nie, N. Yang, and J. Xu, "The development of microstructure of coal by microwave irradiation stimulation," *J. Natural Gas Sci. Eng.*, vol. 66, pp. 86–95, Jun. 2019.

[7] H. Li, B. Lin, W. Yang, C. Zheng, Y. Hong, Y. Gao, T. Liu, and S. Wu, "Experimental study on the petrophysical variation of different rank coals with microwave treatment," *Int. J. Coal Geol.*, vols. 154–155, pp. 82–91, Jan. 2016.

[8] W. Wang, F. Xin, Y. Tu, and Z. Wang, "Pore structure development in Xilingol lignite under microwave irradiation," *J. Energy Inst.*, vol. 91, no. 1, pp. 75–86, Feb. 2018.

[9] H. Li, S. Shi, B. Lin, J. Lu, Q. Ye, Y. Lu, Z. Wang, Y. Hong, and X. Zhu, "Effects of microwave-assisted pyrolysis on the microstructure of bituminous coals," *Energy*, vol. 187, Nov. 2019, Art. no. 115986.

[10] H. Kumar, E. Lester, S. Kingman, R. Bourne, C. Avila, A. Jones, J. Robinson, P. M. Halleck, and J. P. Mathews, "Inducing fractures and increasing cleat apertures in a bituminous coal under isotropic stress via application of microwave energy," *Int. J. Coal Geol.*, vol. 88, no. 1, pp. 75–82, Oct. 2011.

[11] J. Huang, G. Xu, G. Hu, M. Kizil, and Z. Chen, "A coupled electromagnetic irradiation, heat and mass transfer model for microwave heating and its numerical simulation on coal," *Fuel Process. Technol.*, vol. 177, pp. 237–245, Aug. 2018.

[12] H. Li, B. Lin, W. Yang, Y. Hong, and Z. Wang, "A fully coupled electromagnetic-thermal-mechanical model for coalbed methane extraction with microwave heating," *J. Natural Gas Sci. Eng.*, vol. 46, pp. 830–844, Oct. 2017.

[13] H. Li, S. Shi, B. Lin, J. Lu, Y. Lu, Q. Ye, Z. Wang, Y. Hong, and X. Zhu, "A fully coupled electromagnetic, heat transfer and multiphase porous media model for microwave heating of coal," *Fuel Process. Technol.*, vol. 189, pp. 49–61, Jun. 2019.

[14] H. Li, C. Zheng, J. Lu, L. Tian, Y. Lu, Q. Ye, W. Luo, and X. Zhu, "Drying kinetics of coal under microwave irradiation based on a coupled electromagnetic, heat transfer and multiphase porous media model," *Fuel*, vol. 256, Nov. 2019, Art. no. 115966.

[15] B. Lin, H. Li, Z. Chen, C. Zheng, Y. Hong, and Z. Wang, "Sensitivity analysis on the microwave heating of coal: A coupled electromagnetic and heat transfer model," *Appl. Therm. Eng.*, vol. 126, pp. 949–962, Nov. 2017.

[16] Y.-D. Hong, B.-Q. Lin, H. Li, H.-M. Dai, C.-J. Zhu, and H. Yao, ''Three-dimensional simulation of microwave heating coal sample with varying parameters,'' *Appl. Therm. Eng.*, vol. 93, pp. 1145–1154, Jan. 2016.

[17] R. G. Bosisio, J. Spooner, and J. Granger, ''Asphalt road maintenance with a mobile microwave power Unit,'' *J. Microw. Power*, vol. 9, no. 4, pp. 381–386, Jun. 2016.

[18] D. G. Lakins, C. Z. Alvarado, A. M. Luna, S. F. O'Keefe, J. B. Boyce, L. D. Thompson, M. T. Brashears, J. C. Brooks, and M. M. Brashears, ''Comparison of quality attributes of shell eggs subjected to directional microwave technology,'' *Poultry Sci.*, vol. 88, no. 6, pp. 1257–1265, Jun. 2009.

[19] P. T. Nguyen, A. Abbosh, and S. Crozier, ''Microwave hyperthermia for breast cancer treatment using electromagnetic and thermal focusing tested on realistic breast models and antenna arrays,'' *IEEE Trans. Antennas Propag.*, vol. 63, no. 10, pp. 4426–4434, Oct. 2015.

[20] C. O. Kappe, ''Controlled microwave heating in modern organic synthesis,'' *Angew. Chem. Int. Ed.*, vol. 43, no. 46, pp. 6250–6284, Nov. 2004.

[21] T. Uslu and Ü. Atalay, ''Microwave heating of coal for enhanced magnetic removal of pyrite,'' *Fuel Process. Technol.*, vol. 85, no. 1, pp. 21–29, Jan. 2004.

[22] G. Korvin, R. V. Khachaturov, K. Oleschko, G. Ronquillo, M. D. J. Correa López, and J.-J. García, ''Computer simulation of microwave propagation in heterogeneous and fractal media,'' *Comput. Geosci.*, vol. 100, pp. 156–165, Mar. 2017.

[23] M. E. C. Oliveira and A. S. Franca, ''Microwave heating of foodstuffs,'' *J. Food Eng.*, vol. 53, no. 4, pp. 347–359, Aug. 2002.

[24] M. Sharif and M. Zubair, ''Thermodynamics in f (R, T) theory of gravity,'' *J. Cosmol. Astroparticle Phys.*, vol. 2012, no. 3, p. 028, Mar. 2012.

[25] K. Wang, L. Ma, Q. Xiong, S. Liang, G. Sun, X. Yu, Z. Yao, and T. Liu, ''Learning to detect local overheating of the high-power microwave heating process with deep learning,'' *IEEE Access*, vol. 6, pp. 10288–10296, Feb. 2018.

[26] S. Marland, A. Merchant, and N. Rowson, ''Dielectric properties of coal,'' *Fuel*, vol. 80, no. 13, pp. 1839–1849, Oct. 2001.

[27] D. Rittel, ''Experimental investigation of transient thermoelastic effects in dynamic fracture,'' *Int. J. Solids Struct.*, vol. 35, no. 22, pp. 2959–2973, Aug. 1998.

CHANG SU received the master's degree in control theory and control engineering from Liaoning Technical University, in 2007, where she is currently pursuing the Ph.D. degree with the School of Mechanics and Engineering. She is currently a Lecturer with the School of Mechanical Engineering, Liaoning Technical University. Her research interest includes mining of CBM with thermal stimulation and intelligent control.

YONGLI ZHANG received the Ph.D. degree in mining engineering from Liaoning Technical University, in 2000. He is currently a Professor and a Supervisor for the Ph.D. student with the School of Mechanics and Engineering, Liaoning Technical University. He is also the Director of the Fund Management Office, Liaoning Technical University. His research interests include mining disaster mechanics, gas mining, and the theory and application of two-phase fluid.

XINLE YANG received the Ph.D. degree in mechanical engineering from Liaoning Technical University, in 2009. From 2016 to 2017, he was a Visiting Scholar with Industrial Engineering, University of Padova, Italy. He is currently a Professor and a Supervisor for the Ph.D. student with the School of Mechanical Engineering, Liaoning Technical University. His research interests include recovery and power generation in low-grade heat source, and mining of CBM with thermal stimulation.

JUN TU received the Ph.D. degree in system engineering from Northeastern University, in 2014. He is currently an Associate Professor and an Instructor for master's student with the College of Science, Liaoning Technical University. His research interests include mathematics and safety engineering.